

Available online at [www.sciencedirect.com](http://www.sciencedirect.com)

SciVerse ScienceDirect

[www.elsevier.com/locate/jprot](http://www.elsevier.com/locate/jprot)

# Attenuated metabolism is a hallmark of obesity as revealed by comparative proteomic analysis of human omental adipose tissue

Rafael Pérez-Pérez<sup>a, b</sup>, Eva García-Santos<sup>a, b</sup>, Francisco J. Ortega-Delgado<sup>b, c</sup>, Juan A. López<sup>d</sup>, Emilio Camafeita<sup>d</sup>, Wifredo Ricart<sup>b, c</sup>, José-Manuel Fernández-Real<sup>b, c</sup>, Belén Peral<sup>a, b, \*</sup>

<sup>a</sup>Instituto de Investigaciones Biomédicas, Alberto Sols, Consejo Superior de Investigaciones Científicas (CSIC) & Universidad Autónoma de Madrid, E-28029 Madrid, Spain

<sup>b</sup>CIBER Fisiopatología de la Obesidad y Nutrición (CIBEROBN) ISCIII, Spain

<sup>c</sup>Department of Diabetes, Endocrinology and Nutrition, Hospital Dr. Josep Trueta, E-17007 Girona, Spain

<sup>d</sup>Unidad de Proteómica, Centro Nacional de Investigaciones Cardiovasculares (CNIC), E-28029 Madrid, Spain

## ARTICLE INFO

### Article history:

Received 5 August 2011

Accepted 22 September 2011

### Keywords:

2D-DIGE

MALDI-MS

Obesity

Human adipose tissue

TKT

ACY-1

## ABSTRACT

Obesity is recognized as an epidemic health problem worldwide. In humans, the accumulation of omental rather than subcutaneous fat appears to be tightly linked to insulin resistance, type 2 diabetes and cardiovascular disease. Differences in gene expression profiles in the adipose tissue comparing non-obese and obese subjects have been well documented. However, to date, no comparative proteomic studies based on omental fat have investigated the influence of obesity in protein expression. In this work, we searched for proteins differentially expressed in the omental fat of non-obese and obese subjects using 2D-DIGE and MS. Forty-four proteins, several of which were further studied by immunoblotting and immunostaining analyses, showed significant differences in the expression levels in the two groups of subjects. Our findings reveal a clearly distinctive proteomic profile between obese and non-obese subjects which emphasizes: i) reduced metabolic activity in the obese fat, since most down-regulated proteins were engaged in metabolic pathways; and ii) morphological and structural cell changes in the obese fat, as revealed by the functions exerted by most up-regulated proteins. Interestingly, transketolase and aminoacylase-1 represent newly described molecules involved in the pathophysiology of obesity, thus opening up new possibilities in the study of obesity.

© 2011 Elsevier B.V. All rights reserved.

## 1. Introduction

Obesity is one of the most important public health problems facing the world today and has increased dramatically over the last decades in children and adolescents [1]. Obese subjects suffer from decreased life quality and expectancy as well as

increased risk of suffering insulin resistance, type 2 diabetes, cardiovascular disease (CVD), hepatic steatosis, pulmonary and muscular pathologies, psychological disorders and cancer, among others [2]. A person's weight and body composition are likely determined by interaction between his/her genetic make-up and social, cultural, behavioral, and environmental factors.

\* Corresponding author at: Instituto de Investigaciones Biomédicas, Alberto Sols, Consejo Superior de Investigaciones Científicas (CSIC) & Universidad Autónoma de Madrid, Arturo Duperier 4, E-28029 Madrid, Spain. Tel.: +34 915854478; fax: +34 915854401.

E-mail address: [bperal@iib.uam.es](mailto:bperal@iib.uam.es) (B. Peral).

The intake of energy-dense foods, especially when combined with reduced physical activity, is very likely to contribute to the high prevalence of obesity; however, the existence of complex systems that regulate energy balance calls for a broader view of this paradigm [3].

In humans, the adipose tissue is dispersed throughout the body with major intra-abdominal depots around the omentum, intestines, and perirenal areas, as well as in subcutaneous depots in the buttocks, thighs, and abdomen. These two fat depots, the subcutaneous and the omental fat, exhibit unique biochemical and cellular properties, such as response to sex hormones, and different secretion profiles [4], including a different lipolytic program [5]. Moreover, the omental, but not the subcutaneous, fat drains directly into the portal circulation, and some data point out to excessive free fatty acid release from the omental adipose tissue in central obesity [6]. In fact, it is well established that the size of the omental, more than the subcutaneous, fat is strongly related to a higher risk of obesity-related co-morbidities, including insulin resistance, type 2 diabetes, dyslipidemia and CVD. As a consequence of extensive recent investigation, the adipose tissue is no longer regarded a mere fat reservoir, but an endocrine organ which cross-talks with other essential organs like the liver, the muscle, the pancreas, and the brain, being a crucial regulator of whole-body homeostasis.

Gene expression studies (i.e. microarrays and RT-PCR) using adipose tissue from obese and non-obese subjects have yielded important insights into the pathogenesis of obesity and related diseases, (reviewed in [7]). Results pointed out that: i) obesity represents a chronic inflammatory condition, since genes related with inflammation are up-regulated in response to obesity; ii) the differentiation state of obese adipocytes is altered; and iii) the expression of adipogenic genes is decreased in obesity [8–11]. As far as the latter is concerned, it has been suggested that the limited lipogenic and/or adipogenic capacity of obese adipocytes might lead to spillover of excess lipids to other tissues, and lipotoxicity could contribute to the pathogenesis of type 2 diabetes [12].

At the protein level the knowledge about human adipose tissue is limited. A very few proteomic studies have been published using either whole adipose tissue or isolated cells from both fat depots (reviewed in [13]). The majority of these works have studied human adipogenesis or adipose tissue secretome. Recently, however, our group and others have resorted to 2D-DIGE and MS to explore the differences between omental and subcutaneous fat [14–16]. Despite of some drawbacks inherent to 2-DE analysis (mainly the poor representation of low-abundant or very hydrophobic proteins as well as those with extreme pI and molecular weight), the quantitative comparison of proteins in two or more conditions based on 2D-DIGE/MS is a widespread, robust methodology to assess differential protein expression. This approach provides great analytical precision, dynamic range and sensitivity, therefore allowing a reproducible and reliable differential analysis [17]. Nevertheless, to date, no proteomic studies based on omental fat have investigated the influence of obesity in protein expression, given that the omental adipose tissue has been tightly linked to obesity-associated co-morbidities. In this work, we have compared for the first time the omental fat from non-obese and morbidly obese subjects by 2D-DIGE and MS, revealing 44 modulated

proteins in response to obesity. Our findings emphasize a noticeably decreased expression of proteins related to metabolic processes in response to obesity together with a down-regulation of mitochondrial enzymes, which is consistent with a reduced metabolic activity in the obese adipose tissue. In addition, most of the proteins found up-regulated in obesity develop structural functions in the cell, which account for the morphological changes undergone by obese adipocytes. Therefore, our results support a neatly distinctive biological profile in the omental fat of obese and non-obese subjects regarding protein expression.

## 2. Materials and methods

### 2.1. Study design

Omental fat from morbidly obese ( $n=6$ ) and non-obese ( $n=6$ ) subjects obtained during surgery were analyzed by a proteomic approach using 2D-DIGE. Samples were labelled using fluorophore dye-swapping to avoid labelling bias, combined in pairs and separated by electrophoresis. Image analysis revealed modulated proteins which were identified by MS. Results validation was performed by Western Blot with an additional set of subjects. Immunostaining assays were performed to study selected proteins not only in adipose tissue samples, but also in human omental adipocyte cultures. The 3T3-L1 cell line was used to study whether these proteins were modulated in the adipocyte differentiation process.

### 2.2. Biological samples

Omental adipose tissue samples were obtained from 26 women, including 12 non-obese and 14 morbidly obese. Non-obese subjects had a body mass index (BMI)  $<30$  kg/m<sup>2</sup> (BMI ranged from 22.1 to 28.3 kg/m<sup>2</sup>), and age ranged from 25 to 56 years. Morbidly obese subjects had a BMI  $>40$  kg/m<sup>2</sup> (BMI ranged from 40.7 to 48.5 kg/m<sup>2</sup>), and age ranged from 39 to 58 years. All these subjects had been submitted for elective surgical procedures (cholecystectomy, surgery of abdominal hernia and gastric by-pass surgery). During surgery, biopsies of adipose tissues were obtained after an overnight fast, washed in chilled 9 g/L NaCl solution, partitioned into pieces, and immediately frozen in liquid nitrogen and stored at  $-80$  °C until protein extraction. The surgeon aimed to obtain the samples from similar anatomical locations in all the subjects. All women were of Caucasian origin and reported that their body weight had been stable for at least three months before the study. None of the subjects had type 2 diabetes or any other systemic disease apart from obesity and all were free of any infections within the previous month before the study. Liver disease and thyroid dysfunction were specifically excluded by biochemical work-up. Other exclusion criteria for those patients included the following: 1) clinically significant hepatic, neurological, or other major systemic disease, including malignancy; 2) history of drug or alcohol abuse, defined as  $>80$  g/day, or serum transaminase activity more than twice the upper normal range limit; 3) elevated serum creatinine concentrations; 4) acute major cardiovascular event in the previous 6 months; 5) acute illnesses and current evidence of chronic inflammatory

or infectious diseases; and 6) mental illness rendering the subjects unable to understand the nature, scope, and possible consequences of the analysis. The study was conducted according to the recommendations of the Declaration of Helsinki and was approved by the ethics committees of Hospital Dr. Josep Trueta (Girona, Spain). Signed informed consent was obtained from all subjects.

### 2.3. 2D-DIGE analysis

Proteins were extracted from omental adipose tissue biopsies (100 mg) by using the 2D Grinding Kit (GE Healthcare, Uppsala, Sweden) in Lysis Buffer (7 M urea, 2 M thiourea, 4% CHAPS, and 30 mM Tris-HCl pH 8.5) containing 50 mM DTT. The extract was shaken for 30 min at room temperature and centrifuged at 15,000×g for 30 min. Proteins were precipitated with the 2D-CleanUp Kit (GE Healthcare) and redissolved in Lysis Buffer. The protein concentration was determined using RC/DC Protein Assay (Bio-Rad Laboratories, Hercules, CA, USA). Proteins were labelled according to the manufacturer's instruction (GE Healthcare). Briefly, 50 µg of adipose tissue protein extracts was minimally labelled with 400 pmol of the *N*-hydroxysuccinimide esters of Cy3 or Cy5 fluorescent cyanine dyes on ice in the dark for 30 min. All experiments comprised an internal standard containing equal amounts of each cell lysate, which was labelled with Cy2 dye. The labelling reaction was quenched

with 1 µl of 10 mM lysine on ice in the dark for 10 min. The internal standard and the individual omental fat extracts from non-obese and obese subjects were combined and run in a single gel (150 µg total proteins). Proteins extracts were diluted in Rehydration Buffer (7 M urea, 2 M thiourea, 2% CHAPS, 0.8% (v/v) IPG buffer 3-11NL), reduced with 50 mM DTT, and applied by cup-loading to 24 cm IPG strips pH 3-11NL, which were previously rehydrated with Rehydration Buffer containing 100 mM hydroxyethyl disulfide (DeStreak, GE Healthcare). The first and second dimensions together with the equilibration step were performed following the procedure previously described [14].

### 2.4. Image acquisition and analysis

After SDS-PAGE, gels were scanned with a Typhoon 4100 scanner (GE Healthcare) at 100 µm resolution using appropriate individual excitation and emission wavelengths, filters and photomultiplier (PMT) sensitivity for each Cy2, Cy3 and Cy5 dyes (PMT values: 510, 510 and 475 respectively). Gel images were analyzed with the DIA (Differential in-gel Analysis) module of the DeCyder v7 software (GE Healthcare) for automatic spot detection, background subtraction, quantification and normalization with low experimental variation (DeCyder Differential Analysis Software User Manual, version 7; GE Healthcare, 2009). The Biological Variation Analysis (BVA) module utilized those images individually processed with the DIA module to

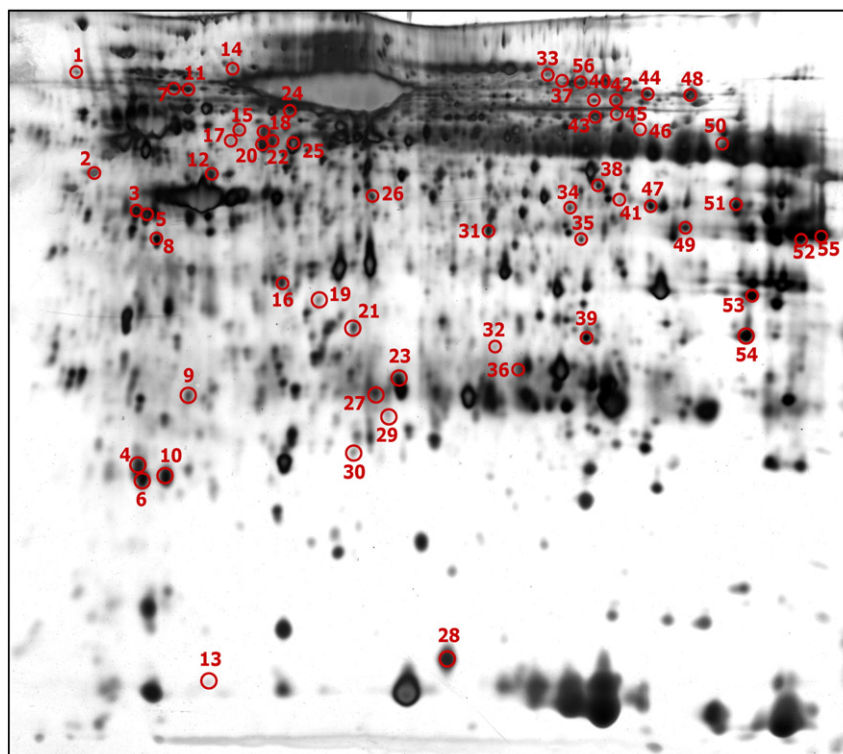


**Fig. 1 – Representative silver stained 2D gel of omental adipose tissue proteins using 24 cm pH3-11NL (left to right) strips in the first dimension and 12% PAGE-SDS gels in the second dimension. Numbers correspond to differentially expressed protein spots as indicated in Table 1. Supplemental Fig. 1 provides a more convenient visualization of the differential protein spots on the silver stained 2D gel.**

**Table 1 – Proteins identified by MALDI-MS showing significantly regulated expression in the omental fat from obese and non-obese individuals.**

DIGE			Protein			Mascot						
Spot <sup>a</sup>	p-value <sup>b</sup>	Av. ratio <sup>c</sup>	Acession <sup>d</sup>	Locus <sup>e</sup>	Name	Score <sup>f</sup>	Expect <sup>g</sup>	Ions score <sup>h</sup>	kDa theor <sup>i</sup>	pI theor <sup>j</sup>	Match pept <sup>k</sup>	Cover % <sup>l</sup>
1	1.6E-02	1.6	gi 642534	AAA85268	Lumican	191	7.90E-13	102	38.7	6.2	5	14
2	8.0E-03	-2.0	gi 62414289	NP_003371	Vimentin	273	4.90E-21		53.7	5.1	19	47
3	1.2E-02	2.2	gi 24234699	NP_002267	Keratin 19	372	6.30E-31	157	44.1	5.0	18	43
4	1.4E-02	2.2	gi 42734430	NP_036364	Polymerase I and transcript release factor	164	3.90E-10	73	43.5	5.5	6	12
5	3.9E-03	2.2	gi 24234699	NP_002267	Keratin 19	257	2.00E-19		44.1	5.0	16	39
6	3.0E-02	1.7	gi 42734430	NP_036364	Polymerase I and transcript release factor	129	2.80E-08	82	43.5	5.5	6	11
7	2.1E-02	1.5	gi 18645167	AAH23990	Annexin A2	136	5.60E-09		38.8	7.6	9	28
			gi 167614506	NP_002289	L-plastin	235	3.10E-17	137	70.8	5.3	11	22
			gi 2897116	AAC39708	Integrin alpha-7	157	2.00E-09	85	125.4	5.6	9	10
			gi 50415798	AAH78178	lamin-B1	129	1.20E-06		38.3	5.4	9	30
8	3.6E-02	2.1	gi 55962552	CAI18465	Heat shock 70 kDa protein 1A	181	7.80E-12	85	52.2	5.4	7	13
9	3.3E-02	1.7	gi 3127926	CAA36267	collagen type VI, alpha 3 chain	89	1.30E-02	91	345.1	6.4	8	3
10	4.2E-02	1.6	gi 42734430	NP_036364	Polymerase I and transcript release factor	157	2.00E-09	74	43.5	5.5	6	12
11	5.5E-03	1.8	gi 62898171	BAD97025	L-plastin variant	240	9.90E-18	103	70.8	5.2	10	18
12	2.0E-02	1.6	gi 119626083	EAX05678	Albumin, isoform CRA_t	168	1.60E-10		60.2	6.7	14	27
13	1.2E-02	2.1	gi 4506925	NP_003013	SH3 domain binding glutamic acid-rich protein like	87	4.60E-04	69	12.8	5.2	1	8
14	4.7E-02	1.4	gi 42476013	NP_940916	NHL repeat containing 2	114	3.90E-05	57	80.2	5.3	4	6
15	6.3E-03	2.6	gi 25777732	NP_000681	Mitochondrial aldehyde dehydrogenase 2 precursor	312	6.30E-25	149	56.9	6.6	11	22
16	4.3E-02	-1.5	gi 91992949	AAI14619	Guanine nucleotide-binding protein beta subunit	161	7.80E-10	77	37.1	5.6	5	16
17	3.0E-02	1.6	gi 181573	AAA35763	Cytokeratin 8	147	2.00E-08	82	53.5	5.5	5	10
18	5.8E-05	2.7	gi 67782365	NP_005547	Keratin 7	293	4.90E-23	133	51.4	5.4	15	30
19	2.2E-02	1.5	gi 4096652	AAC99987	Aryl sulfotransferase	102	1.40E-05	82	34.3	5.8	1	3
20	2.7E-03	2.0	gi 2781209	1FZA_C	Fibrinogen gamma chain	240	9.90E-18	128	36.5	5.9	7	33
21	3.1E-02	1.9	gi 4502101	NP_000691	Annexin I	187	2.00E-12	105	38.9	6.6	5	17
22	3.1E-03	2.3	gi 1419564	CAA67203	Keratin 8, isoform CRA_d	115	3.10E-05	81	30.8	5.0	2	8
23	1.9E-03	-2.1	gi 662841	AAA62175	Heat shock protein 27	126	2.50E-06	93	22.4	7.8	2	13
24	4.8E-03	1.6	gi 168988718	2VDB_A	Serum albumin	161	7.80E-10		67.8	5.6	12	18
25	1.1E-03	2.6	gi 237823916	3GHG_C	Chain C, human fibrinogen	396	2.50E-33	216	47.0	5.5	14	51
			gi 181573	AAA35763	Cytokeratin 8	366	2.50E-30	186	53.5	5.5	15	37
26	2.0E-03	-1.5	gi 4501901	NP_000657	Aminoacylase 1	190	9.90E-13	60	46.1	5.8	8	18
27	1.6E-03	1.5	gi 18645167	AAH23990	Annexin A2	185	3.10E-12	69	38.8	7.6	7	20
28	1.2E-02	-1.7	gi 4557581	NP_001435	Fatty acid binding protein 5 (psoriasis-associated)	277	2.00E-21	88	15.5	6.6	10	68

29	3.1E-02	1.8	gi 119626066	EAX05661	Albumin, isoform CRA_c	141	7.80E-08		27.7	6.4	8	30
30	4.4E-02	1.9	gi 17389815	AAH17917	Triosephosphate isomerase 1	131	7.80E-07		26.9	6.5	7	32
31	1.1E-02	-1.7	gi 4557233	NP_000008	Short-chain acyl-CoA dehydrogenase precursor	119	1.20E-05		44.6	8.1	7	19
32	3.9E-02	-1.5	gi 157168362	NP_000261	Nucleoside phosphorylase	123	4.90E-06	71	32.3	6.5	3	14
33	3.1E-02	-1.8	gi 110590599	2HAV_A	Serotransferrin precursor	119	1.20E-05		77.0	6.9	9	17
34	6.3E-03	-1.5	gi 4557231	NP_000007	Medium-chain acyl-CoA dehydrogenase isoform a precursor	158	1.60E-09	91	47.0	8.6	4	13
35	2.1E-03	-1.5	gi 119631279	EAX10874	3-hydroxyisobutyryl-coenzyme A hydrolase, isoform CRA_b	159	1.20E-09		49.4	9.4	9	23
36	3.2E-02	-1.5	gi 4502517	NP_001729	Carbonic anhydrase I	141	1.80E-09	72	28.9	6.6	4	21
37	3.1E-02	1.4	gi 27436946	NP_733821	Lamin A/C isoform 1 precursor	521	7.80E-46	232	74.4	6.6	22	38
38	4.8E-03	-1.5	gi 119590499	EAW70093	Fumarate hydratase, isoform CRA_d	174	3.90E-11	136	46.6	6.9	2	6
39	6.0E-05	-1.7	gi 189181759	NP_001121188	electron transfer flavoprotein, alpha polypeptide isoform b	167	4.50E-12	93	30.2	8.8	4	20
40	4.3E-02	-1.4	gi 4557735	NP_000231	Monoamine oxidase A	126	2.50E-06	69	60.2	7.9	4	11
41	1.0E-02	-1.9	gi 30583667	AAP36082	Citrate synthase	109	1.20E-04	69	29.6	7.8	2	7
42	1.1E-02	-1.6	gi 71296885	AAH44787	Monoamine oxidase A	146	2.50E-08	66	60.2	6.9	6	15
43	4.3E-03	-1.4	gi 4557014	NP_001743	Catalase	278	1.60E-21	115	59.9	6.9	9	25
44	1.3E-02	-1.5	gi 388891	AAA61222	Transketolase	150	9.90E-09		68.5	7.9	10	22
45	3.2E-03	-1.6	gi 179950	AAB59522	Catalase	195	3.10E-13	70	51.6	7.8	8	23
46	3.1E-03	-1.8	gi 223002	0401173A	Fibrin beta	170	9.90E-11		51.4	8.0	10	26
47	1.4E-04	-1.6	gi 48257138	AAH00105	Citrate synthase, mitochondrial precursor	211	7.80E-15	101	45.8	6.5	6	16
48	3.0E-02	-1.7	gi 388891	AAA61222	Transketolase	178	1.60E-11		68.5	7.9	10	25
49	1.0E-02	-1.5	gi 4557237	NP_000010	Acetyl-coenzyme A acetyltransferase 1 precursor	129	1.20E-06	95	45.5	9.0	2	7
50	8.8E-03	-1.5	gi 13111901	AAH03119	ATP synthase subunit alpha, mitochondrial precursor	101	1.80E-05	86	40.4	8.9	1	3
51	1.8E-02	-1.4	gi 16950633	NP_446464	Argininosuccinate synthetase 1	180	9.90E-12	49	46.8	8.1	7	16
52	1.7E-02	-1.7	gi 598143	AAB48003	Alcohol dehydrogenase beta-3 subunit	220	9.90E-16		40.7	8.5	12	32
53	2.7E-02	2.0	gi 4757756	NP_004030	Annexin A2 isoform 2	283	4.90E-22	87	38.8	7.6	15	48
54	1.9E-02	-1.6	gi 119626625	EAX06220	L-3-hydroxyacyl-coenzyme A dehydrogenase short chain isoform CRA_c	170	9.90E-11	78	7.6	9.3	4	52
55	4.1E-02	-1.6	gi 598143	AAB48003	Alcohol dehydrogenase beta-3 subunit	212	6.20E-15	63	40.7	8.5	10	28
56	3.5E-02	-1.5	gi 40807491	NP_001986	Acyl-CoA synthetase long-chain family member 1	306	2.50E-24	141	78.9	6.8	11	20

<sup>a</sup>Spot numbering as shown in 2-DE silver gel in Fig. 1. <sup>b</sup>p-value of the Student's t test and <sup>c</sup>average volumen ratio (obese/non-obese) as calculated by the DeCyder analysis. <sup>d</sup>Protein and <sup>e</sup>locus accession codes from the NCBI database. <sup>f</sup>Mascot score, <sup>g</sup>Mascot expected value, <sup>h</sup>Mascot ion score, <sup>i</sup>theoretical molecular weight (kDa) and <sup>j</sup>pI, <sup>k</sup>number of matched peptides and <sup>l</sup>protein sequence coverage for the most probable candidate as provided by Mascot. Protein identification details (MS and MS/MS spectra) are listed in Supplemental Table 1.

<sup>a</sup>Spot numbering as shown in 2-DE silver gel in Fig. 1. <sup>b</sup>p-value of the Student's t test and <sup>c</sup>average volumen ratio (obese/non-obese) as calculated by the DeCyder analysis. <sup>d</sup>Protein and <sup>e</sup>locus accession codes from the NCBI database. <sup>f</sup>Mascot score, <sup>g</sup>Mascot expected value, <sup>h</sup>Mascot ion score, <sup>i</sup>theoretical molecular weight (kDa) and <sup>j</sup>pI, <sup>k</sup>number of matched peptides and <sup>l</sup>protein sequence coverage for the most probable candidate as provided by Mascot. Protein identification details (MS and MS/MS spectra) are listed in Supplemental Table 1.

match protein spots across gels, using the internal standard for gel-to-gel matching. Statistical analysis was then carried out to determine protein expression changes. *P*-values lower than 0.05 as calculated from Student's *t* test were considered significant. Multivariate analysis was performed by Principal Components Analysis (PCA) using the algorithm included in the Extended Data Analysis (EDA) module of the DeCyder software based on the spots matched across all gels.

### 2.5. In-gel trypsin digestion and mass spectrometry

Protein spots showing significantly altered expression levels in the 2 groups of samples by DeCyder Software were selected for gel excision from silver-stained gels, digested automatically on a Proteiner DP robot (Bruker Daltonik, Bremen, Germany) using the protocol of [18] and analyzed in an Ultraflex MALDI TOF/TOF mass spectrometer (Bruker Daltonik) [19] to obtain the corresponding MALDI-MS and MALDI-MS/MS spectra. In a first step, MALDI-MS spectra were acquired by averaging 300 individual spectra in the positive ion reflector mode at 50 Hz laser frequency in a mass range from 800 to 4000 Da. In a second step, precursor ions showing in the MALDI-MS mass spectrum were subjected to fragment ion analysis in the tandem (MS/MS) mode to average 1000 spectra. Peak labelling, internal calibration based on two trypsin autolysis ions with  $m/z=842.510$  and  $m/z=2211.105$ , as well as removal of known trypsin and keratin peptide masses were performed automatically using the flexAnalysis 2.2 software (Bruker Daltonik). No smoothing or any further spectral processing was applied. MALDI-MS and MS/MS spectra were manually inspected in detail and reacquired, recalibrated and/or relabelled using the aforementioned programs and homemade software when necessary.

### 2.6. Database searching

MALDI-MS and MS/MS data were combined through the BioTools 3.0 program (Bruker Daltonik) to search a nonredundant protein database (NCBI nr 20091022;  $\sim 7.0 \times 10^6$  entries; National Centre for Biotechnology Information, Bethesda, USA), using the Mascot 2.2 software (Matrix Science, London, UK; <http://www.matrixscience.com>) [20]. Other relevant search parameters were set as follows: enzyme, trypsin; fixed modifications, carbamidomethyl (C); allow up to 1 missed cleavage; peptide tolerance  $\pm 20$  ppm; MS/MS tolerance  $\pm 0.5$  Da. Protein scores greater than 81 were considered significant ( $p < 0.05$ ).

### 2.7. Cell culture and adipocyte differentiation

Isolated human omental pre-adipocytes (Zen-Bio, Inc. Raleigh, NC, USA) were cultured with omental pre-adipocytes medium (Zen-Bio, Inc.) at 37 °C and 5% CO<sub>2</sub> and differentiated using omental differentiation medium (Zen-Bio, Inc.) according to the method outlined by Ortega et al. [21]. Two weeks after the initiation of differentiation, cells appeared rounded with large lipid droplets in the cytoplasm and were considered mature adipocytes. Murine 3T3-L1 fibroblasts (CCL 92.1, American Type Culture Collection) were grown to confluence in DMEM containing 10% calf serum. The differentiation to adipocytes was induced according to the procedure described by Ortega et

al. [21]. On days 0, 3, 5 and 9, three replicated cell samples were separately collected for later immunoassays.

### 2.8. Immunoblotting analysis

Fat tissue or cultured cells were homogenized in radioimmuno precipitation assay (RIPA) buffer as described in [14]. Protein extracts (ca. 10  $\mu$ g) were loaded, resolved on SDS-PAGE and transferred to Hybond ECL nitrocellulose membranes by conventional procedures. Membranes were stained with 0.15% Ponceau red (Sigma-Aldrich, St Louis, MO, USA) to ensure equal loading after transfer and then blocked with 5% (w/v) BSA or dried nonfat milk in TBS buffer with 0.1% Tween 20. The antibodies used for Western Blot analysis revealed in each case single bands at the expected molecular masses. The primary antibodies used were: 1:2000 rabbit anti-TKT (HPA029480), and 1:2000 rabbit anti-ACY-1 (A6609) (Sigma-Aldrich); 1:2000 goat anti-Beta-actin (sc-1616); 1:4000 rabbit anti-SPHK1 (sc-48825), and 1:200 goat anti-FABP5 (sc-16060) (Santa Cruz Biotechnology); 1:1000 mouse anti-HSP70 (C92F3A-5) (Stressgen Bioreagents); 1:500 rabbit anti-FABP4 (Eurogentec, Seraing, Belgium). Blots were incubated with the appropriate IgG-HRP-conjugated secondary antibody. Immunoreactive bands were visualized with ECL-plus reagent kit (GE Healthcare). Blots were exposed for different times; exposures in the linear range of signal were selected for densitometric evaluation. Optical densities of the immunoreactive bands were measured using Image J analysis software. Statistical comparisons of the densitometry data were carried out using the Student's *t* test for samples, and results were expressed as means  $\pm$  standard deviation (SD) using SPSS 16.0 (SPSS Inc., Illinois, USA). Statistical significance was set at  $p < 0.05$ .

### 2.9. Immunohistochemistry

Five-micron sections of formalin-fixed paraffin-embedded adipose tissue were deparaffinised and rehydrated prior to antigen unmasking by boiling in 1 mM EDTA, pH 8. Sections were blocked in normal serum and incubated overnight with rabbit anti-TKT (1:500 dilution) or rabbit anti-ACY-1 (1:200 dilution) antibodies. Secondary antibody staining was performed using the VECTASTAIN ABC kit (Vector Laboratories, Inc. Burlingame, CA) and detected with diaminobenzidine (DAB, Vector Laboratories, Inc.). Sections were counterstained with hematoxylin prior to dehydration and coverslip placement, and examined under a Nikon Eclipse 90i microscope. As a negative control, the procedure was performed in the absence of primary antibody.

### 2.10. Immunofluorescence

Frozen adipose tissue sections or cultured cells were fixed with 4% paraformaldehyde and permeabilized for 30 min with 0.1% Triton X-100 in PBS. Staining was performed overnight at 4 °C with rabbit anti-TKT (1:500 dilution) or with rabbit anti-ACY-1 (1:400 dilution) antibodies, washed, and visualized using Alexa Fluor 546 goat anti-rabbit antibody (1:500; Molecular Probes Inc., OR, USA). The slides were counterstained with DAPI (4,6-diamidino-2-phenylindole) to reveal nuclei. The lipophilic fluorescence dye BODIPY 493/503 was used for lipid droplet labelling according to the manufacturer's instruction (Molecular Probes Inc.). The slides were examined under a Leica TCS SP5

fluorescent microscope (Heidelberg, Germany). As a negative control, the assay was performed in the absence of primary antibody.

### 3. Results

#### 3.1. Proteomic analysis of obese and non-obese adipose tissue samples

To detect proteins differentially expressed in obesity, omental fat samples from morbidly obese ( $n=6$ ) and non-obese ( $n=6$ ) females were analyzed by 2D-DIGE. Protein extracts were labelled using dye-swapping with either Cy3 or Cy5 fluorescent dye to avoid labelling bias arising from the fluorescence properties of gels at different wavelengths. Then each Cy3/Cy5-labelled sample pair was mixed with a Cy2-labelled internal standard and loaded onto each gel. After 2-DE, the Cy2, Cy3 and Cy5 channels were individually imaged from each gel (Supplemental Fig. 1). Automated image analysis performed with DeCyder software detected approximately 2700 spots per gel in the 3–11 NL pH range with a molecular mass of 10–150 kDa, of which 1200 spots were matched throughout all gels. Multivariate PCA showed that the “non-obese group” was efficiently discriminated from the “obese group” (data not shown). DeCyder statistical analyses showed that 70 protein spots were differentially expressed at  $p<0.05$  considering only those spots present in all gels. These spots were excised from silver-stained gels, digested with trypsin, and analyzed by MALDI-MS followed by database search. Fifty-six spots, which corresponded to 44

unique proteins could be identified (Fig. 1 and Table 1). Twenty proteins were increased and 24 decreased in response to obesity.

#### 3.2. Functional classification of the proteins differentially expressed

To understand the biological relevance of protein expression changes in response to obesity, the Protein Analysis Through Evolutionary Relationship (PANTHER) application (<http://www.pantherdb.org/>) was used. This classification system uses information on protein sequence to assign a gene to an ontology group on the basis of the Gene Ontology (GO) terms <http://www.geneontology.org/>. Thus, the two sets of up- and down-regulated proteins were searched for significantly over-represented ( $p<0.05$ ) GO terms. Two key Biological Process classes were found significantly enriched in the group of down-regulated proteins: *Metabolic Process* and *Generation of Precursor Metabolites and Energy*, while three key Biological Process classes (*Cellular Process*, *Developmental Process* and *Cellular Component Organization*) were significantly enriched in the set of up-regulated proteins. Likewise, the categorization based on the Molecular Function GO category showed that most down-regulated proteins accounted for one key significant class, *Catalytic Activity*, while *Structural Molecule Activity* revealed as the unique key GO term with significant enrichment in the up-regulated proteins from obese adipose tissue (Fig. 2).

In addition, PANTHER application mapped the 44 differentially expressed proteins into parent and child categories with regard to their Molecular Function and Biological Process GO

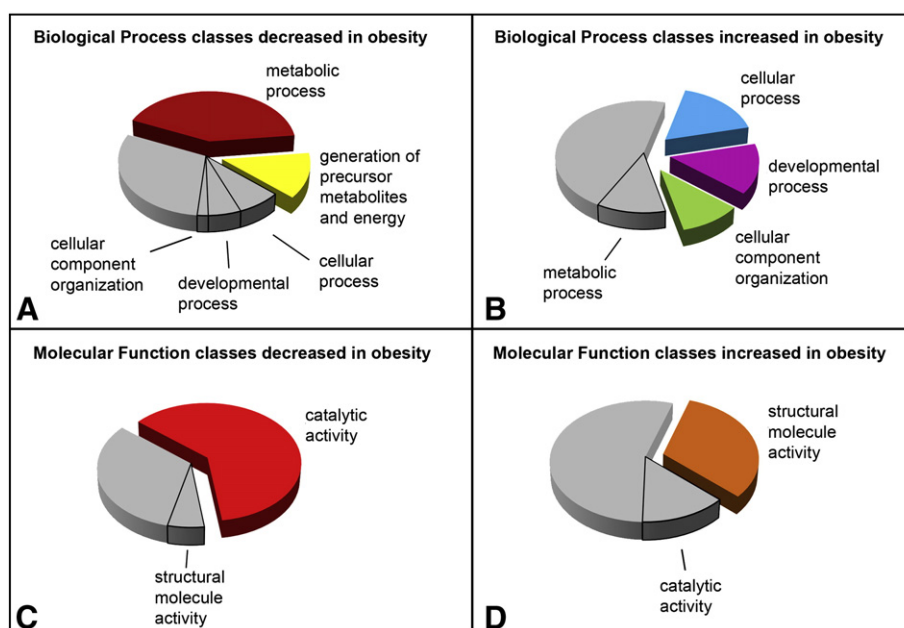


**Fig. 2** – Pie chart representations of PANTHER Biological Process and Molecular Function classes significantly over-represented in the set of downregulated proteins (A, C) and in the set of up-regulated proteins (B, D) in obesity. Classes with no significant *P*-value are displayed in grey colour for comparative purposes (note that the class *Generation of Precursor Metabolites and Energy* has no representation in the group of proteins increased in obesity). It should be pointed that PANTHER may attribute multiple classes to a given protein.

terms (Supplementary Table 2), highlighting that most of the down-regulated proteins were engaged in metabolic pathways. Our results have also revealed that the set of down-regulated proteins comprised numerous (14 out of 24, 58%) mitochondrial enzymes, overall supporting a reduced metabolic activity in the obese adipose tissue.

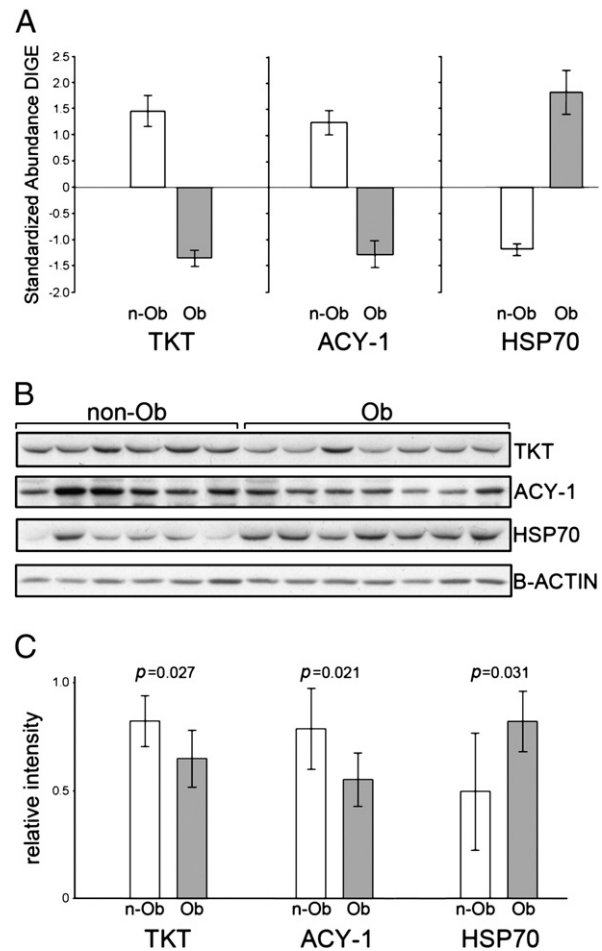
### 3.3. Validation of differential protein expression

Western Blot analyses were performed in an additional set of non-obese and morbidly obese women for two proteins whose expression in human adipose tissue had not been previously documented, TKT and ACY-1, together with two molecules, HSP70 and FABP5 that had been earlier studied in fat and/or in obesity and related co-morbidities. One of these proteins was shown up-regulated (HSP70) and the other three were found down-regulated (TKT, ACY-1 and FABP5) in response to obesity. Immunoblotting analysis using an antibody against TKT confirmed that this protein was over-expressed ( $p < 0.05$ ) in the non-obese group of subjects, confirming 2-DE findings (Fig. 3). Likewise, ACY-1 levels were significantly more abundant ( $p < 0.05$ ) in the non-obese subjects (Fig. 3), in agreement with 2D-DIGE results. Both TKT and ACY-1 were studied by immunostaining methods, as well as in the adipocyte differentiation process. Immunoblotting analysis revealed that HSP70 was significantly increased in obese vs. non-obese individuals ( $p < 0.05$ ), thus confirming 2D-DIGE results (Fig. 3). By using an antibody anti-FABP5, immunoblotting analysis revealed an over-expression of FABP5 protein in the omental adipose tissue from non-obese compared to obese subjects; however this result did not reach statistical significance ( $p = 0.06$ ) mostly due to the high SD observed in non-obese samples (data not shown). It must be noted that Western Blot assay may fail to validate particular protein isoforms found differentially expressed by 2D-DIGE/MS as they rely on antibodies lacking the necessary specificity.

### 3.4. Immunostaining analyses

Immunohistochemical and immunofluorescence approaches were performed to determine the cellular distribution of TKT and ACY-1 proteins in biopsies of omental fat given that, as far as we know, these proteins have not been earlier analyzed in this tissue. TKT was assayed in sections of omental adipose tissue by both techniques revealing similar results. Immunofluorescence detection showed a bright staining pattern mainly in the cytoplasm of adipocytes and of stromal-vascular fraction (SVF) cells, as well as in the nuclei of a few cells (Fig. 4A). To determine whether the stained nuclei pertained to adipocytes, immunofluorescence analysis from a cellular culture of human pre-adipocytes and differentiated adipocytes was performed. This analysis showed that in pre-adipocytes TKT was localized in the cytoplasm as well as in the nucleus, while in adipocytes only the cytoplasm but not the nucleus was stained (Fig. 4B and C). TKT expression was also confirmed in adipose tissue macrophages by co-staining assays using CD68 (not shown).

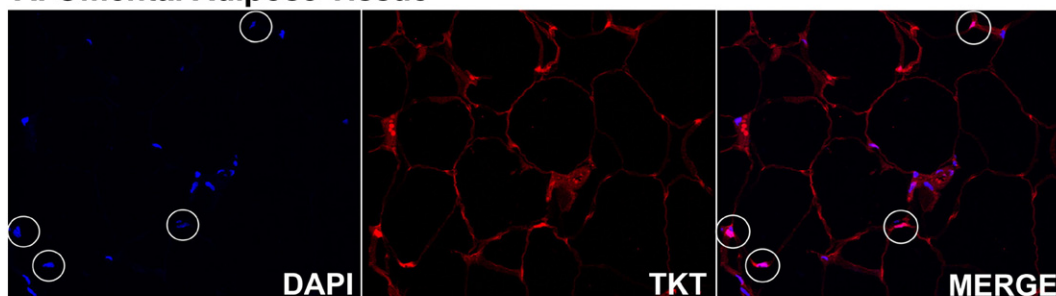
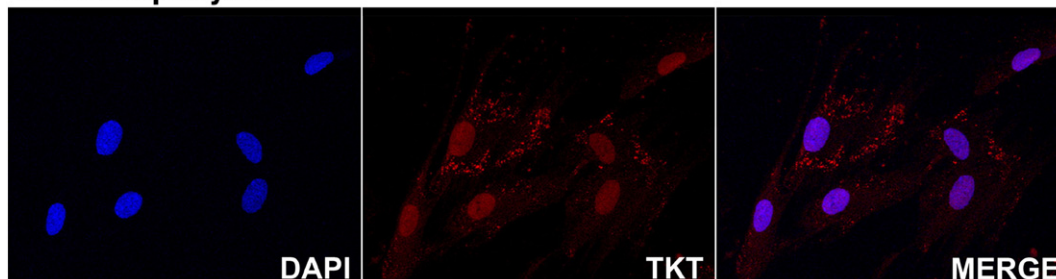
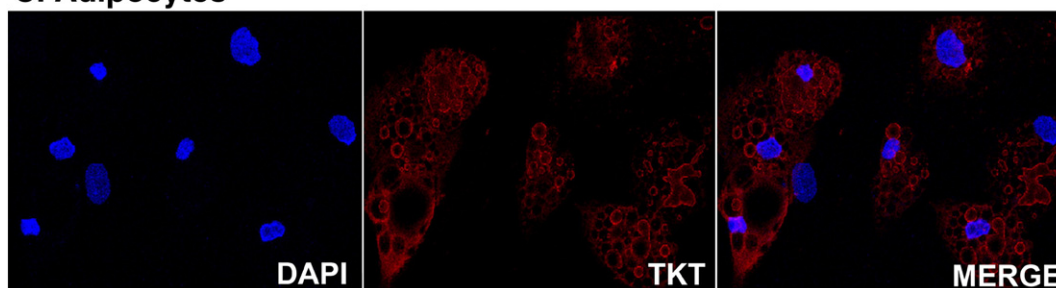
ACY-1 was also assayed in sections of omental fat by immunostaining analyses, which showed that ACY-1 was expressed in the cytoplasm as well as in the nucleus of



**Fig. 3 – TKT, ACY-1 and HSP70 expression in human omental adipose tissue. Standardized abundance was determined by DeCyder analysis of 2D-DIGE data from non-obese and obese fat samples. The (+) and (-) symbols indicate increased and decreased levels with respect to the internal standard, respectively (A). Representative Western Blot analysis of TKT, ACY-1 and HSP70 expression from non-obese and obese fat samples. The results were normalized for B-actin density (B). Values for relative intensity obtained after densitometry of the bands are means  $\pm$  SD (C). Representative images of four independent analyses.**

adipocytes and SVF cells, including omental mesothelial cells (Supplemental Fig. 2A and 2B). Immunofluorescence analysis revealed the presence of ACY-1 in the nucleus of cultured human omental pre-adipocytes (Fig. 5A), while in differentiated adipocytes ACY-1 localized around cytosolic lipid droplets and, to a lesser extent, in the nucleus (Fig. 5B and 5C). In addition, we had also performed immunofluorescence analysis in 3T3-L1 cells during the adipogenic process. As illustrated in Supplemental Fig. 3A, ACY-1 was localized exclusively in 3T3-L1 fibroblast nuclei (day 0), as was the case for human pre-adipocytes; however, in 3T3-L1 differentiated adipocytes (day 9), ACY-1 was shown around lipid droplets in the cytoplasm, as well as in the majority of the nuclei (Supplemental Fig. 3B and 3C).



**A. Omental Adipose Tissue****B. Preadipocytes****C. Adipocytes**

**Fig. 4** – Immunofluorescence staining of TKT in human omental adipose tissue, human pre-adipocytes and human adipocytes differentiated *in vitro*. In fat biopsies TKT is mainly shown in the cytosol of adipocytes and other SVF cells, but is also observed in the nuclei of a few cells (four white circles) (A). In human pre-adipocytes TKT is shown both in the cytoplasm and the nucleus (B). In human differentiated adipocytes TKT is exclusively observed in the cytosol (C). Images are representative of adipose tissue sections collected from three subjects (A) and three replicates (B and C).

### 3.5. 3T3-L1 adipogenesis

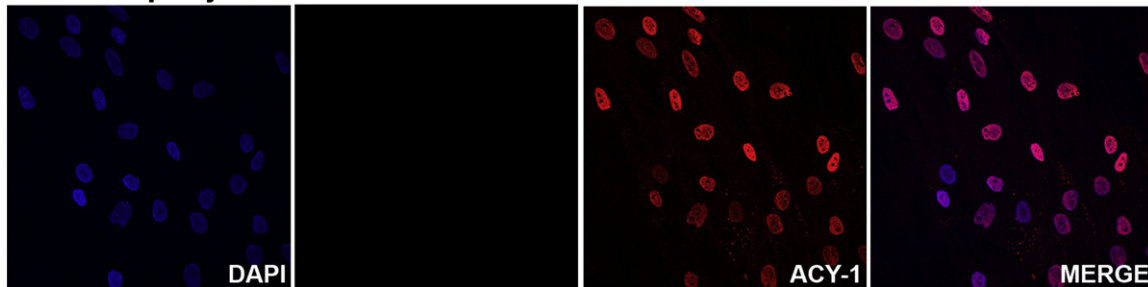
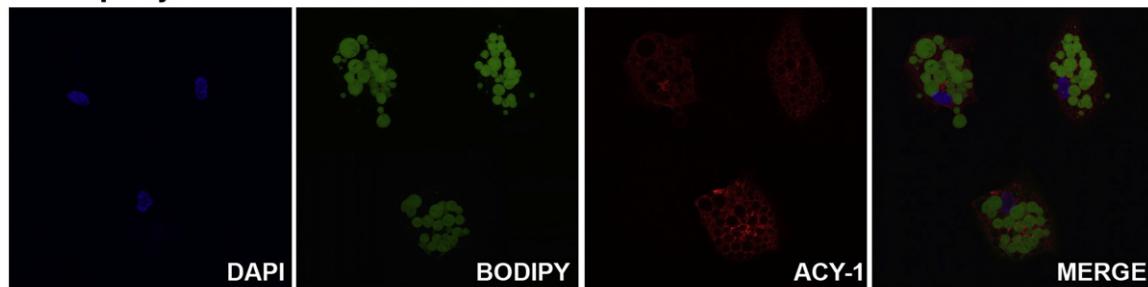
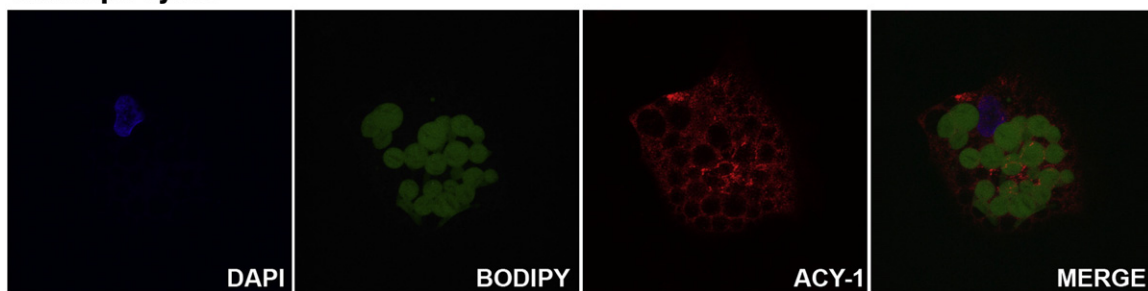
To further study TKT and ACY-1 proteins, we performed immunoblotting analysis with proteins extracted during the adipogenic maturation of 3T3-L1 cells using the previously described specific antibodies. TKT and ACY-1 were significantly augmented with adipocyte differentiation in parallel to the expression of FABP4, which was used as an adipogenesis control (Fig. 6).

## 4. Discussion

Over the last years an increasing number of studies have focused in the analysis of gene expression to gain insight into obesity and related pathologies. However only a few number of studies have resorted to proteomic methods to identify human fat proteins associated to these disorders. In the present study we have employed a proteomic approach based on 2D-DIGE and MALDI-MS to uncover differences in protein expression using biopsies of omental fat from non-obese and

morbidly obese individuals, reporting for the first time a set of 44 proteins that are significantly modulated in these two sets of subjects. Our study has focused on omental adipose tissue as this fat depot has been long associated with augmented risk of suffering pathologies related to obesity [22].

The down-regulation of proteins related to metabolic processes such as *Amino Acid Metabolism*, *Carbohydrate Metabolism* and *Lipid Metabolism* suggests a reduction of metabolic activity in the obese omental fat, and is consistent with previous mRNA studies [8–10, 23]; thus, Ortega *et al.* [10] demonstrated the down-regulation of the main lipogenic enzymes in obese omental fat using a large cohort of individuals. In this scenario, these findings provide evidence for an impaired capacity of the adipose tissue to function as an energy reservoir. In addition, it is noteworthy the high number of mitochondrial enzymes included in the set of down-regulated proteins in the obese adipose tissue, 14 proteins out of 24, which is consistent with the reduction in the oxidative metabolism in obesity. Our findings are in agreement with previous microarray analysis revealing a coordinated down-regulation of catabolic pathways operating in the mitochondria such as: fatty acid B

**A. Preadipocytes****B. Adipocytes****C. Adipocytes**

**Fig. 5 – Immunofluorescence staining of ACY-1 in human omental pre-adipocytes and adipocytes differentiated *in vitro*. ACY-1 (in red) is shown in the nucleus of pre-adipocytes (day 0) (A). In differentiated adipocytes (day 14) ACY-1 is observed in the cytosol and to a lesser extent in the nucleus (B). Close-up view of a differentiated adipocyte showing ACY-1 around the lipid droplets (C). The counterstaining of nuclei (DAPI) is shown in blue. Lipid droplets have been stained with BODIPY 493/503 (in green). Images are representative of three replicates. (For interpretation of the references to colour in this figure legend, the reader is referred to the web version of this article.)**

oxidation, tricarboxylic acid cycle and electron transport chain [24]. In addition, a strong correlation between impaired adipocyte mitochondrial activity and/or content and obesity has been well documented [25–27]. Decreased mitochondrial capacity in adipocytes may alter adipocyte insulin sensitivity and/or function due to the high energetic requirements for fatty acid storage, adipokine secretion [28], insulin signalling [29], and glucose uptake. Therefore, the relatively high number of mitochondrial proteins found down-regulated in our study is consistent with previous evidences.

The set of up-regulated proteins, which pertain to the following significantly enriched classes: *Cellular Process*, *Developmental Process*, *Cellular Component Organization*, and *Structural Molecule Activity*, suggests that the enlargement of the obese adipocytes, by increasing fat storage, is accompanied by: i) cytoskeleton changes, such as alteration of LMNA, LMNB1 and integrin alpha 7; ii) changes in the extracellular matrix (ECM), such as collagen (COL6A3) and lumican; and iii) tissue structure modifications, such as alteration in epithelial cyto-keratins, CK-7, CK-8 and CK-19, compatible with omental

mesothelium changes. Our findings showing the up-regulation of proteins controlling cell architecture and tissue remodelling are in agreement with previous transcriptomic studies reporting that the expansion of adipose tissue is associated with a remodelling of ECM together with changes of fat cell cytoskeleton [23, 30] compatible with the need to adapt fat pads as adiposity increase.

Several relevant proteins highlighted by our study were more in-depth analyzed. Transketolase (TKT) expression levels were reduced in obese patients. To our knowledge this is the first time that a link between TKT and obesity is reported. This protein is a thiamine diphosphate (ThDP)-dependent enzyme that catalyzes several reactions in the non-oxidative branch of the Pentose Phosphate Pathway (PPP). In mammalian cells, the main function of PPP is to produce the reduced form of nicotinamide-adenine dinucleotide phosphate (NADPH), which functions in detoxification processes and lipid biosynthesis. Another function of PPP is to convert hexose into pentose, which is required for nucleic acid synthesis [31]. TKT haploinsufficient mice showed a markedly

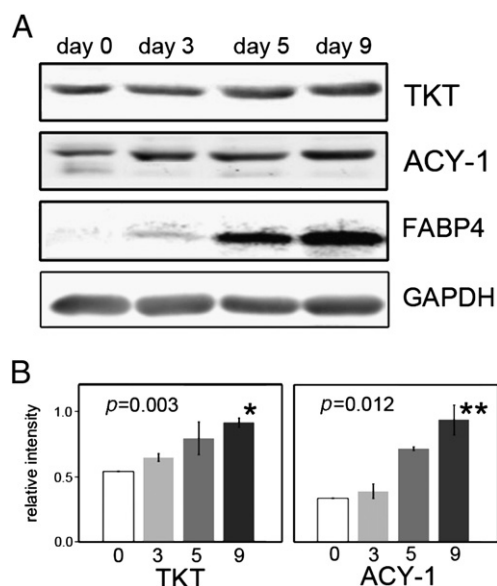


**Fig. 6 – TKT and ACY-1 and protein levels assessed by Western Blot during adipogenic maturation of 3T3-L1 (A). Values for relative intensity obtained after densitometry of the bands are means  $\pm$  SD. \*  $p < 0.005$  and \*\*  $p < 0.05$  for comparisons between TKT, and ACY-1 levels at day 9 vs. day 0, respectively (B). FABP4 was used as an adipogenesis control. The results were normalized for GAPDH density. Representative images of three independent analyses.**

reduction in adipose tissue (77%) [32] which could be induced by NADPH deficiency, limiting the production of lipids in the fat. The reduced levels of TKT found in the group of obese vs. non-obese subjects could be explained by the occurrence of a compensatory mechanism through which the obese adipose tissue would prevent further enlargement. In this scenario, during the period of dynamic obesity large amounts of NADPH are required for fatty acid biosynthesis, and an increase in TKT function is expected. In contrast, it is well known that lipogenic pathways are reduced in established obesity [10] and TKT down-regulation could be a late and adaptive process, aimed at limiting a further development of fat mass. Immunostaining methods showed for the first time the expression of TKT in human omental adipose tissue. TKT, an ubiquitous enzyme engaged in multiple metabolic pathways, was widely distributed in adipocytes as well as other stromal cells. TKT was present mainly in the cytoplasm of adipose cells, but a few nuclei also expressed the protein. Interestingly, the nuclei of human pre-adipocytes expressed TKT in contrast to fully differentiated adipocytes, in which TKT was only observed in the cytoplasm. A nuclear localization of TKT had already been described [33]; in this regard, it is interesting to mention that in a highly proliferative state increased cell division rate would require large amounts of phosphate pentose, which would account for the nuclear localization of TKT. On the other hand, mature adipocytes keep pentose phosphate consumption to a minimum while consuming many NADPH molecules for lipogenesis, which would explain TKT localization in the cytoplasm of mature adipocytes. Taken together, these findings highlight the potential role of this protein in adipose tissue and adipogenesis.

2D-DIGE and immunoblotting analyses have shown significant down-regulation of aminoacylase-1 (ACY-1) with obesity. ACY-1 is a cytosolic, homodimeric, zinc-binding enzyme that function in the catabolism and retrieval of acylated amino acids. ACY-1 expression has been found associated to renal carcinoma [34] and to an inborn metabolic disorder [35]. Nevertheless, this is the first report on ACY-1 expression in human fat. The nuclear localization of ACY-1 is striking. In agreement with our finding, this enzyme had been previously found in the nucleus of rat normal proximal tubular cells [34]. It is possible that several unidentified nuclear proteins are substrates for ACY-1. It is noteworthy that ACY-1 physically interacts and functionally modulates sphingosine kinase 1, SPHK1 [36], a lipid kinase that converts sphingosine and ATP to sphingosine-1-phosphate (S1P). S1P is a potent signalling molecule involved in angiogenesis and cell growth among other cellular processes [37]. Of note, we have shown that both ACY-1 and SPHK1 are associated with adipogenesis in 3T3-L1 cells (Fig. 6 and Supplemental Fig. 4) as already found with the latter [38]. These results collectively support the hypothesis that the SPHK1/ACY-1 system could play a role in obesity. Further studies are underway to explore ACY-1 functional role in adipose tissue.

Our results based on the 3T3-L1 adipocytes differentiation process have shown for the first time an increment of ACY-1 and TKT levels. Long-lasting fat excess has been evidenced to reduce adipogenesis in adipose tissue to limit further expansion of fat mass [8–11]. We hypothesize that the diminished levels of ACY-1 and TKT proteins in obesity stem from the impaired adipogenic capacity of obese adipocytes.

The proteomic analysis has enabled the identification of other relevant proteins involved in obesity or whose expression in fat has been widely documented. Results revealed the over-expression in obese subjects of HSP70. HSPs not only serve as chaperones, mainly controlling protein folding of newly translated polypeptides but also protect cells against many chronically and acutely stressful conditions [39]. In spite of the numerous cellular processes in which HSP70 takes part, it can be hypothesized that the higher levels of HSP70 found in the omental fat from obese patients would serve to reduce the cellular stress associated to obesity. In skeletal muscle, evidences have shown that there is a decreased expression of HSP70 in type 2 diabetes patients [40, 41] and in mice models an elevation of HSP70 protected against obesity-induced hyperglycemia, hyperinsulinemia, glucose intolerance and insulin resistance [41]. Nevertheless, no similar studies have been conducted in adipose tissue to date. We performed Western Blot analyses to compare omental fat samples from obese patients with and without type 2 diabetes. Interestingly, in agreement with these evidences, our results revealed that the amount of HSP70 was significantly lower in type 2 diabetes obese subjects than in obese without type 2 diabetes ( $p = 0.007$ ), as illustrated in Supplemental Fig. 5. Therefore this result supports a protection role for HSP70.

It is well established that monoamine oxidase A (MAOA), a mitochondrial enzyme involved in the oxidative deamination catabolism of neurotransmitters and exogenous amines, is highly expressed in the adipocyte-enriched fraction of human adipose tissue [42]. Our results showed reduced levels of MAOA in obese subjects, which is in agreement with an earlier report revealing reduced MAOA activity in the adipose tissue from obese subjects [43]. Our study also showed reduced

expression levels of FABP5 in obese individuals, in consistency with previous studies in subcutaneous fat [44]. FABP5 is a relevant adipose tissue protein that facilitates lipid usage in metabolic pathways and plays a role in metabolic syndrome, insulin resistance, type 2 diabetes, and atherosclerosis, as elucidated in studies based on genetically modified mice [45]. Mice lacking FABP5 was protected against diet-induced obesity, insulin resistance and other related diseases [46]. Ongoing studies in our laboratory attempt to evaluate whether these results might be extrapolated to humans.

In summary, this work is, to our knowledge, the first proteomic study on omental fat comparing non-obese and obese people and represents one of the few proteomic analyses in human adipose tissue. Our findings evidence a clearly distinctive biological profile of obese and non-obese subjects highlighting a noticeably decreased expression of proteins related to metabolic processes and an increased expression of proteins that develop structural functions in the cell in response to obesity. Besides, our study has revealed that TKT and ACY-1 are promising new players involved in obesity. Our results will strengthen the understanding of molecular pathogenesis of obesity, whilst the identified proteins can be regarded as potential targets for future therapeutic strategies.

Supplementary materials related to this article can be found online at [doi:10.1016/j.jprot.2011.09.016](https://doi.org/10.1016/j.jprot.2011.09.016).

## Acknowledgements

This work was supported by Grants SAF-2009-10461 (to B.P.), SAF-2008-02073 (to J.M.F.R.) from the Ministerio de Ciencia e Innovación de España and from the Fundación Mutua Madrileña (to B.P.). The CNIC is supported by the Ministerio de Ciencia e Innovación and the Pro CNIC Foundation. CIBER is an initiative from the Instituto de Salud Carlos III. We acknowledge the technical assistance of Ana de la Encarnación, Pablo Parra and Alba Moratalla.

## REFERENCES

- Daniels SR, Jacobson MS, McCrindle BW, Eckel RH, Sanner BM. American Heart Association Childhood Obesity Research Summit Report. *Circulation* 2009;119:e489-517.
- Calle EE, Kaaks R. Overweight, obesity and cancer: epidemiological evidence and proposed mechanisms. *Nat Rev Cancer* 2004;4:579-91.
- Spiegelman BM, Flier JS. Obesity and the regulation of energy balance. *Cell* 2001;104:531-43.
- Montague CT, O'Rahilly S. The perils of portliness: causes and consequences of visceral adiposity. *Diabetes* 2000;49:883-8.
- Rebuffe-Scrive M, Andersson B, Olbe L, Bjorntorp P. Metabolism of adipose tissue in intraabdominal depots of nonobese men and women. *Metabolism* 1989;38:453-8.
- Matsuzawa Y. Therapy insight: adipocytokines in metabolic syndrome and related cardiovascular disease. *Nat Clin Pract Cardiovasc Med* 2006;3:35-42.
- Keller MP, Attie AD. Physiological insights gained from gene expression analysis in obesity and diabetes. *Annu Rev Nutr* 2010;30:341-64.
- Nadler ST, Stoehr JP, Schueler KL, Tanimoto G, Yandell BS, Attie AD. The expression of adipogenic genes is decreased in obesity and diabetes mellitus. *Proc Natl Acad Sci U S A* 2000;97:11371-6.
- Gomez-Ambrosi J, Catalan V, Diez-Caballero A, Martinez-Cruz LA, Gil MJ, Garcia-Foncillas J, et al. Gene expression profile of omental adipose tissue in human obesity. *FASEB J* 2004;18:215-7.
- Ortega FJ, Mayas D, Moreno-Navarrete JM, Catalan V, Gomez-Ambrosi J, Esteve E, et al. The gene expression of the main lipogenic enzymes is downregulated in visceral adipose tissue of obese subjects. *Obesity (Silver Spring)* 2010;18:13-20.
- Dubois SG, Heilbronn LK, Smith SR, Albu JB, Kelley DE, Ravussin E. Decreased expression of adipogenic genes in obese subjects with type 2 diabetes. *Obesity (Silver Spring)* 2006;14:1543-52.
- Wang MY, Grayburn P, Chen S, Ravazzola M, Orci L, Unger RH. Adipogenic capacity and the susceptibility to type 2 diabetes and metabolic syndrome. *Proc Natl Acad Sci U S A* 2008;105:6139-44.
- Peral B, Camafeita E, Fernandez-Real JM, Lopez JA. Tackling the human adipose tissue proteome to gain insight into obesity and related pathologies. *Expert Rev Proteomics* 2009;6:353-61.
- Perez-Perez R, Ortega-Delgado FJ, Garcia-Santos E, Lopez JA, Camafeita E, Ricart W, et al. Differential proteomics of omental and subcutaneous adipose tissue reflects their unlike biochemical and metabolic properties. *J Proteome Res* 2009;8:1682-93.
- Peinado JR, Jimenez-Gomez Y, Pulido MR, Ortega-Bellido M, Diaz-Lopez C, Padillo FJ, et al. The stromal-vascular fraction of adipose tissue contributes to major differences between subcutaneous and visceral fat depots. *Proteomics* 2010;10:3356-66.
- Kheterpal I, Ku G, Coleman L, Yu G, Ptitsyn AA, Floyd ZE, et al. Proteome of human subcutaneous adipose tissue stromal vascular fraction cells versus mature adipocytes based on DIGE. *J Proteome Res* 2011;10:1519-27.
- Corton M, Botella-Carretero JI, Lopez JA, Camafeita E, San Millan JL, Escobar-Morreale HF, et al. Proteomic analysis of human omental adipose tissue in the polycystic ovary syndrome using two-dimensional difference gel electrophoresis and mass spectrometry. *Hum Reprod* 2008;23:651-61.
- Shevchenko A, Tomas H, Havlis J, Olsen JV, Mann M. In-gel digestion for mass spectrometric characterization of proteins and proteomes. *Nat Protoc* 2006;1:2856-60.
- Suckau D, Resemann A, Schuerenberg M, Hufnagel P, Franzen J, Holle A. A novel MALDI LIFT-TOF/TOF mass spectrometer for proteomics. *Anal Bioanal Chem* 2003;376:952-65.
- Perkins DN, Pappin DJ, Creasy DM, Cottrell JS. Probability-based protein identification by searching sequence databases using mass spectrometry data. *Electrophoresis* 1999;20:3551-67.
- Ortega FJ, Vazquez-Martin A, Moreno-Navarrete JM, Bassols J, Rodriguez-Hermosa J, Girones J, et al. Thyroid hormone responsive Spot 14 increases during differentiation of human adipocytes and its expression is down-regulated in obese subjects. *Int J Obes (Lond)* 2010;34:487-99.
- Despres JP, Lemieux I. Abdominal obesity and metabolic syndrome. *Nature* 2006;444:881-7.
- Henegar C, Tordjman J, Achard V, Lacasa D, Cremer I, Guerre-Millo M, et al. Adipose tissue transcriptomic signature highlights the pathological relevance of extracellular matrix in human obesity. *Genome Biol* 2008;9:R14.
- Marrades MP, Gonzalez-Muniesa P, Arteta D, Martinez JA, Moreno-Aliaga MJ. Orchestrated downregulation of genes involved in oxidative metabolic pathways in obese vs. lean high-fat young male consumers. *J Physiol Biochem* 2011;67:15-26.
- Wilson-Fritch L, Burkart A, Bell G, Mendelson K, Leszyk J, Nicoloso S, et al. Mitochondrial biogenesis and remodeling

- during adipogenesis and in response to the insulin sensitizer rosiglitazone. *Mol Cell Biol* 2003;23:1085–94.
- [26] Rong JX, Qiu Y, Hansen MK, Zhu L, Zhang V, Xie M, et al. Adipose mitochondrial biogenesis is suppressed in db/db and high-fat diet-fed mice and improved by rosiglitazone. *Diabetes* 2007;56:1751–60.
- [27] Patti ME, Corvera S. The role of mitochondria in the pathogenesis of type 2 diabetes. *Endocr Rev* 2010;31:364–95.
- [28] Koh EH, Park JY, Park HS, Jeon MJ, Ryu JW, Kim M, et al. Essential role of mitochondrial function in adiponectin synthesis in adipocytes. *Diabetes* 2007;56:2973–81.
- [29] Shi X, Burkart A, Nicoloso SM, Czech MP, Straubhaar J, Corvera S. Paradoxical effect of mitochondrial respiratory chain impairment on insulin signaling and glucose transport in adipose cells. *J Biol Chem* 2008;283:30658–67.
- [30] Poussin C, Hall D, Minehira K, Galzin AM, Tarussio D, Thorens B. Different transcriptional control of metabolism and extracellular matrix in visceral and subcutaneous fat of obese and rimonabant treated mice. *PLoS One* 2008;3:e3385.
- [31] Schenk G, Duggleby RG, Nixon PF. Properties and functions of the thiamin diphosphate dependent enzyme transketolase. *Int J Biochem Cell Biol* 1998;30:1297–318.
- [32] Xu ZP, Wawrousek EF, Piatigorsky J. Transketolase haploinsufficiency reduces adipose tissue and female fertility in mice. *Mol Cell Biol* 2002;22:6142–7.
- [33] Joshi S, Singh AR, Kumar A, Misra PC, Siddiqi MI, Saxena JK. Molecular cloning and characterization of Plasmodium falciparum transketolase. *Mol Biochem Parasitol* 2008;160:32–41.
- [34] Zhong Y, Onuki J, Yamasaki T, Ogawa O, Akatsuka S, Toyokuni S. Genome-wide analysis identifies a tumor suppressor role for aminoacylase 1 in iron-induced rat renal cell carcinoma. *Carcinogenesis* 2009;30:158–64.
- [35] Sass JO, Mohr V, Olbrich H, Engelke U, Horvath J, Fliegauf M, et al. Mutations in ACY1, the gene encoding aminoacylase 1, cause a novel inborn error of metabolism. *Am J Hum Genet* 2006;78:401–9.
- [36] Maceyka M, Nava VE, Milstien S, Spiegel S. Aminoacylase 1 is a sphingosine kinase 1-interacting protein. *FEBS Lett* 2004;568:30–4.
- [37] Allende ML, Yamashita T, Proia RL. G-protein-coupled receptor S1P1 acts within endothelial cells to regulate vascular maturation. *Blood* 2003;102:3665–7.
- [38] Hashimoto T, Igarashi J, Kosaka H. Sphingosine kinase is induced in mouse 3T3-L1 cells and promotes adipogenesis. *J Lipid Res* 2009;50:602–10.
- [39] Calderwood SK, Khaleque MA, Sawyer DB, Ciocca DR. Heat shock proteins in cancer: chaperones of tumorigenesis. *Trends Biochem Sci* 2006;31:164–72.
- [40] Kurucz I, Morva A, Vaag A, Eriksson KF, Huang X, Groop L, et al. Decreased expression of heat shock protein 72 in skeletal muscle of patients with type 2 diabetes correlates with insulin resistance. *Diabetes* 2002;51:1102–9.
- [41] Chung J, Nguyen AK, Henstridge DC, Holmes AG, Chan MH, Mesa JL, et al. HSP72 protects against obesity-induced insulin resistance. *Proc Natl Acad Sci U S A* 2008;105:1739–44.
- [42] Pizzinat N, Marti L, Remaury A, Leger F, Langin D, Lafontan M, et al. High expression of monoamine oxidases in human white adipose tissue: evidence for their involvement in noradrenaline clearance. *Biochem Pharmacol* 1999;58:1735–42.
- [43] Visentin V, Prevot D, De Saint Front VD, Morin-Cussac N, Thalamas C, Galitzky J, et al. Alteration of amine oxidase activity in the adipose tissue of obese subjects. *Obes Res* 2004;12:547–55.
- [44] Fisher RM, Hoffstedt J, Hotamisligil GS, Thorne A, Ryden M. Effects of obesity and weight loss on the expression of proteins involved in fatty acid metabolism in human adipose tissue. *Int J Obes Relat Metab Disord* 2002;26:1379–85.
- [45] Furuhashi M, Hotamisligil GS. Fatty acid-binding proteins: role in metabolic diseases and potential as drug targets. *Nat Rev Drug Discov* 2008;7:489–503.
- [46] Maeda K, Cao H, Kono K, Gorgun CZ, Furuhashi M, Uysal KT, et al. Adipocyte/macrophage fatty acid binding proteins control integrated metabolic responses in obesity and diabetes. *Cell Metab* 2005;1:107–19.